Reviewer #1 (egusphere-2025-6493)

Summary and overall assessment

The manuscript presents a strong observational analysis of refractory black carbon (rBC) in the central Arctic marine boundary layer during the ATWAICE (PS131) campaign, with a specific emphasis on warm air-mass intrusions (WAIs) and their influence on rBC size, coating thickness, and absorption enhancement. The study is timely and relevant given the increasing frequency of WAIs and their implications for Arctic aerosol-radiation interactions.

The work is scientifically sound, the dataset is valuable, and the interpretation is largely well supported. The minor revisions needed are:

(i) improved clarity around interpretation boundaries (source vs. processing, morphology vs. coating effects),

(ii) strengthened contextualization and framing for absorption enhancement retrievals, and (iii) a figure/presentation fixe-most notably Figure 4b, where overlapping text reduces readability and must be corrected.

Recommendation: I would strongly recommend to publish this study as a research article in ACP with suggested minor revisions.

We thank the reviewer for detailed evaluation, positive comments and fruitful suggestions. We have revised the manuscript considering all the comments and suggestions from the reviewer. Below, we provide our responses (in bold blue letters) to all the queries raised by the reviewer, which are also incorporated in the revised manuscript.

Comments

1) Low absorption enhancement during WA1: clarify source vs. processing attribution

The manuscript shows that WA1 is associated with larger rBC cores but lower coating thickness and lower E_{abs} relative to "pristine" regimes. The interpretation currently risks reading as "limited coating → low E_{abs}" as the dominant mechanism.

Why this needs tightening:

For Arctic transport events, source-type differences (biomass burning vs. flaring vs. anthropogenic) and particle-scale heterogeneity (morphology, internal structure, compositional mixing) can influence lensing behavior and the validity of idealized core–shell assumptions used in Mie-based calculations.

Requested action:

Add explicit wording that the observed low E_{abs} during WA1 may reflect a combination of:

limited atmospheric aging and coating growth (processing constraint), and source-related differences in rBC composition and morphology that can make core–shell Mie lensing less effective or less representative.

Response:

We thank the reviewer for highlighting the need to more clearly separate processing related versus source-related controls on the low absorption enhancement (E_{abs}) observed during WA1. We agree that interpreting the result solely as "limited coating → low Eabs" can be narrow, particularly for Arctic transport events where source-type differences and particle-scale heterogeneity (e.g., morphology, internal structure, compositional mixing) may alter lensing behaviour and reduce the representativeness of idealized core-shell assumptions used in Mie-based approaches. We have therefore revised the text to explicitly state that the low E_{abs} during WA1 likely reflects a combination of (i) limited atmospheric aging/coating and (ii) source-related differences in rBC composition/morphology that can make core-shell lensing less effective or less representative.

The following text has been added to the revised manuscript:

"Although reduced coating thickness during WA1 is consistent with lower absorption enhancement (E_{abs}), caution should be taken against interpreting WA1 as being controlled solely by a 'limited coating to low E_{abs}' mechanism. For Arctic transport events, the observed E_{abs} likely reflects a combination of constrained atmospheric processing (limited aging and coating) and source-related differences in rBC properties. In particular, differences in rBC composition, morphology/internal structure, and particle-scale mixing heterogeneity can reduce absorption efficiency and/or make core-shell Mie-based representations less effective or less representative."

2) Figure 4b presentation issue (required fix)

Figure 4, panel (b) requires modification or recomposition, as text overlaps on the bar chart, making labels difficult to read and potentially ambiguous. While this is a production-level issue, it affects scientific clarity.

Response: Complied with. We revised Figure 4b by replacing with a time-series representation of the major chemical species and their mass concentrations (Figure 5) according to the suggestions by reviewer 2.

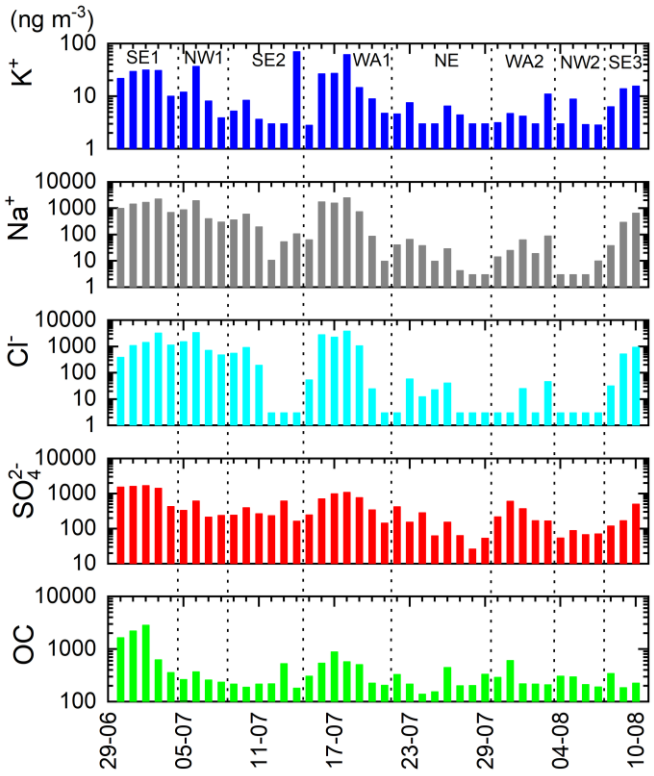

Figure 5: Mass concentration of major chemical species such as OC, SO_4^{2-}, Cl^-, Na^+ and K^+ measured during the study period.

3) Chemical interpretation: daily PM_{10} filters vs. submicron rBC mixing state

The manuscript appropriately notes that PM_{10} filter composition does not directly represent the coating composition on submicron rBC cores measured by SP2. However, some interpretive statements still rely on PM_{10}-derived sulfate and OC fractions.

Requested action:

Insert one explicit sentence stating that links between bulk chemical composition and rBC coating thickness are qualitative and should not be interpreted as direct coating composition closure. Where sulfate/OC fractions are used, frame them as supportive consistency rather than mechanistic proof.

Response: We thank the reviewer for this important clarification. We agree that the daily PM_{10} filter composition represents bulk aerosol chemical composition and cannot be directly linked to the coating composition on submicron rBC cores measured by the SP2.

We have revised the text to make this limitation explicit and to avoid over-interpretation: To avoid over-interpretation, we have revised the relevant text to explicitly state that any links between bulk chemical composition (e.g., PM_{10} derived sulfate and OC fractions), and rBC coating thickness are qualitative and should not be interpreted as a quantitative indicator of rBC coating.

The following text has been added to the revised manuscript:

"The PM_{10} chemical composition reflects bulk aerosol composition integrated over a 24-h period and across a broad size range, its relationship to SP2-derived submicron rBC coating thickness is qualitative; therefore, sulfate and OC fractions should not be interpreted as quantitative indicators of rBC coating."

4) Missing fraction of rBC

I would recommend to add a sentence regarding the missing fraction of rBC considered in this study.

Response: Complied with. The following sentence has been added to the revised manuscript.

In this study, the rBC mass concentration was corrected for the missing fraction of rBC (6 ± 4 %) due to the detection limit of SP2.

5) Comparison with marine environments

Strengthen comparison with recent marine-environment studies (e.g., Pan et al., 2026 and similar recent literature), focusing on rBC concentrations and size distributions.

If feasible include a summary table with mean and median values comparing rBC mass concentration and MMD. This addition would significantly improve the broader relevance and interpretability of the results.

Response:

We thank the reviewer for this valuable suggestion. We agree that a broader comparison with marine-environment studies would improve the contextual relevance of our findings. In the revised manuscript, we have expanded the discussion to compare our observed rBC mass concentrations and size distributions with those reported in recent marine/coastal/remote regions, including Pan et al. (2026) and other relevant literature. This comparison helps place our observations within the wider range of marine/remote atmospheric conditions and highlights similarities and differences in rBC loading and microphysical characteristics across regions. Following the reviewer's recommendation, we have also included a summary table of rBC mass concentrations and MMD from our study and selected studies from other environments.

Accordingly, the following text has been added to the Section 3.2.

"Earlier studies have shown that summertime Arctic rBC is generally characterized by very low background concentrations, with occasional enhancements linked to transport. Taketani et al. (2016) reported pronounced spatial variability between the North Pacific and Arctic oceans in September, with rBC mass concentrations ranging from 0 to 60 ng m^{-3} and an average of

about 1 ng m^{-3}, while Schulz et al. (2019) observed that combustion particles constituted only a minor fraction of the aerosol population in the Canadian Arctic during summer, with near-surface rBC concentrations typically below 2 ng m^{-3}, reflecting weak exchange between the summer polar dome and mid-latitude air masses. In the present study, most air-mass regimes, including NW 1, NW2, SE2, SE3, and NE, exhibited similarly low mean rBC concentrations of about 1.4-1.6 ng m^{-3} 3, with median values of 0.5-0.8 ng m^{-3}, indicating that these conditions represent the clean summertime Arctic background. Our observed rBC concentrations are also lower than those reported by Liu et al. (2015) in the European Arctic during spring, where rBC mass concentrations ranged from 20 to 100 ng m^{-3}, as expected from the seasonal transition from the spring Arctic haze period to the comparatively cleaner summer atmosphere. At the same time, the elevated concentrations observed during south easterly 1 (48.7 ± 49.8 ng m^{-3}; median 36.8 ng m^{-3}) and the two warm-air intrusion cases (11 ± 14.4 and 5.1 ± 8.3 ng m^{-3}) demonstrate that episodic transport can still substantially perturb this otherwise low-rBC environment. These enhanced values are comparable to or approach those reported at Arctic receptor sites such as Pallas, Finland (26 ng m^{-3}; Raatikainen et al., 2015) and Zeppelin, Svalbard (39 ± 23 ng m^{-3}; Zanatta et al., 2018), but remain far lower than those reported for marine and continental regions outside the Arctic, including the remote Antlantic Ocean(~100 ng m^{-3}) (Pan et al. 2026), south-eastern Arabian Sea (938 ± 293 ng m^{-3}), northern Indian Ocean (546 ± 80 ng m^{-3}), equatorial Indian Ocean (206 ± 114 ng m^{-3}) (Kompalli et al., 2021), Thumba (670 ± 571 ng m^{-3}; Nithin et al., 2026), Mukteshwar in the Himalayas (1000 ± 600 ng m-3; Raatikainen et al., 2017), and Lulang on the Tibetan Plateau (310 ± 550 ng m-3; Wang et al., 2018). Table 1 summarizes our observed MrBC values in comparison with those reported in previous studies from marine, remote, coastal environments."

Also, the following text has been revised in the Section 3.3.

"The MMD values observed during this campaign are within the broad range reported previously for Arctic and other remote environments, although substantial variability exists across regions and airmass transport regimes. In the present study, MMD ranged from ~156 nm during SE1 to ~264 nm during WA1, whereas the Arctic background regimes were characterized by MMD around 190-227 nm. These values are comparable to those reported for the Arctic Ocean in summer (~170 nm; Taketani et al. (2016), Pallas in the Finnish Arctic (161-231 nm; Raatikainen et al., 2015), and Zeppelin during spring (Zanatta et al. 2018), but are higher thatn the 119-134 nm reported for the high Canadian Arctic by Schulz et al. (2019). Previous studies from other remote and coastal environments similarly show a wide spread, including 140 nm at Melpitz (Yang et al., 2025), 153-170 nm at Catalina Island (Ko et al. 2020), 200-220 nm at Fukue Island (Shiraiwa et al., 2008), and ~192 nm at Thumba (Nithin et al. 2026). These comparisons indicate that the MMD values measured in this study are generally high relative to those reported for other marine/remote/coastal environments."

Table 1: rBC mass concentration and mass median diameters reported in this study and the values available from previous studies in the marine/remote/coastal regions.

Location/Region	rBC mass concentration (ng m^{-3})		Mass median diameter (nm)	Reference
	Mean ± SD	Median		
Marine environments				
South easterly 1	48.7 ± 49.8	36.8	156	Present study
North westerly 1	1.4 ± 3	0.6	207	Present study
North westerly 2	1.6 ± 2.5	0.8	217	Present study
South easterly 3	1.6 ± 3	0.8	218	Present study
South easterly 2	1.6 ± 3	0.5	190	Present study
North easterly	1.4 ± 2.7	0.6	227	Present study
Warm airmass intrusion 1	11 ± 14.4	3.4	264	Present study
Warm airmass intrusion 2	5.1 ± 8.3	1.6	220	Present study
Pallas, Finnish Arctic	26		161-231	Raatikainen et al. (2015)
Arctic Ocean	1 ± 1.2		~170	Taketani et al. (2016)
Zeppelin, Arctic	39 ± 23		240	Zanatta et al. (2018)
Alert	22 ± 13		160 - 180	Sharma et al. (2017)
Southern Ocean	0.14			Fossum et al. (2022)
South-eastern Arabian Sea	938 ± 293		190	Kompalli et al. (2021)
Northern Indian Ocean	546 ± 80		200	Kompalli et al. (2021)
Equatorial Indian Ocean	206 ± 114		190	Kompalli et al. (2021)
Remote Antlantic	100		180	Pan et al. (2026)
Remote environments				
Jungfraujoch, Switzerland	13.24	1.4 - 20.5	220-240	Liu et al. (2010)
Lulang, Tibetan Plateau, China	310± 550		160	Wang et al. (2018)
Mukteshwar, the Himalayas, India	1000 ± 600		205	Raatikainen et al. (2017)
North-eastern Qinghai–Tibetan Plateau, China	160 ± 190		187	Wang et al. (2015)
Melpitz	160		140	Yang et al. (2025)

Fukue Island Japan	160 ± 50	200 -220	Shiraiwa et al. (2008)
Catalina Island	40 ± 10	153 - 170	Ko et al. (2020)
Coastal sites			
Thumba	670 ± 571	192	Nithin et al. (2026)
Mace Head	3.31		Fossum et al. (2022)

Supplement integration

The supplement provides important context for meteorology and EC variability. Consider adding one sentence in the main text explicitly directing readers to the relevant supplementary figures for context.

Response: Complied with.

Terminology and consistency

Use one consistent spelling of air mass / air-mass / airmass throughout.

Ensure consistent use of "rBC" vs. "BC" when referring specifically to SP2-derived refractory black carbon.

Response: Complied with.

Interpretation balance relative to prior work

Where the manuscript contrasts its findings with earlier studies, consider phrasing such as "in contrast to" rather than language implying inconsistency or error. Briefly noting differences in season, meteorology, or boundary-layer regime will strengthen the comparison.

Response: Thank you for this helpful suggestion. We have revised the relevant text to use more balanced phrasing, such as "in contrast to", instead of wording that could imply inconsistency or error in earlier studies. We also briefly note that differences in season, meteorological conditions, and boundary-layer regime may contribute to the differing results, which strengthens the comparison and places our findings in a more appropriate context relative to prior work.

Reviewer #2 (egusphere-2025-6493)

This manuscript presents rBC concentrations measured by SP2 in the Arctic Ocean and carefully explains the relationship between the concentrations, cover thickness, and temperature and trajectories. The rBC observation data in the Arctic are valuable, interesting, and appropriately processed. However, there are many less substantiated suggestions and insufficient discussion, making the manuscript overall redundant and hindering understanding of the important measurement results. Furthermore, as noted in the comments below, there are several deficiencies and errors in the discussion. If these are sufficiently improved, I can recommend publication.

We thank the reviewer for detailed evaluation, positive comments and fruitful suggestions. We have revised the manuscript considering all the comments and suggestions from the reviewer. Below, we provide our responses (in bold blue letters) to all the queries raised by the reviewer, which are also incorporated in the revised manuscript.

Major comments

1. Eabs: This paper calculates Eabs under the assumption of a core-shell (presumably spherical) structure. However, many previous studies have already shown that the lensing effect calculated for a core-shell structure is overestimated compared to that of actual particles with complex shapes and mixing states, based on model calculations and Eabs observations (e.g., doi:10.1029/2009JD012868, doi:10.5194/acp-16-2525-2016, doi:10.1021/acs.est.5c10094). Therefore, I believe that the Eabs calculated for a core-shell structure are not of sufficient quality to be used in other studies. However, I think it is acceptable to use it in the study to discuss the causes of the difference. The authors should take this into account when discussing Eabs. Therefore, the authors should refer to the multiple previous studies listed above and state that the estimated values differ from the observed values. Furthermore, in the abstract, I recommend that this value should either be deleted or noted that it was calculated assuming a core-shell structure.

Response: We thank the reviewer for this important comment. We agree that absorption enhancement (E_{abs}) estimated using core-shell morphology can overestimate lensing relative to real atmospheric black carbon particles, which often exhibit complex morphology and mixing state.

As noted by the reviewer, several studies have showed that core-shell based Mie calculations can yield higher E_{abs} than observed or than predicted by more realistic morphologies and mixing state representations (Adachi et al., 2010; Ueda et al., 2016; Wu et al. 2018; Zhang et al. 2026). In the revised manuscript, we have therefore: explicitly acknowledged this limitation and clarified that our E_{abs} values are Mie model estimated under a core-shell assumption for single rBC particles measured using SP2 and may differ from observed E_{abs} for ambient particles. Further, we have revised the abstract stated that the reported E_{abs} is calculated assuming a core-shell structure using Mie theory.

The following text has been added to the revised manuscript.

Section 2.2:

"The light absorption enhancement (E_{abs}) estimated here is using an idealized spherical, concentric core-shell representation (Mie theory based). It should be noted that real atmospheric BC commonly exhibits complex/fractal morphology and heterogeneous mixing/coating structures, for which core-shell Mie representations can overestimate E_{abs} values that differ from those inferred from morphology-resolving calculations and observations (e.g., Adachi et al., 2010; Ueda et al., 2016; Fierce et al., 2020; Wang et al., 2021; Zhang et al. 2026). Therefore, absolute E_{abs} values should be interpreted cautiously."

Section 3.5:

"It is important to note that the E_{abs} values reported here are based on a core-shell Mie theory that assumes a spherical BC core fully encapsulated by non-absorbing coating material. Ambient rBC particles, however, often exhibit fractal/irregular morphologies, partial coating, and substantial mixing state heterogeneity. As a result, core-shell-based E_{abs} may represent an upper-bound or idealized estimate of absorption enhancement relative to more realistic particle representations (e.g., Adachi et al., 2010; Ueda et al., 2016; Fierce et al., 2020; Liu et al., 2020; Zhai et al., 2022; Romshoo et al., 2025)."

2. 3 Result and discussion: The section is redundant (especially 3.1). While the details are provided in the Specific Comments, many sentences lack sufficient evidence. I recommend reducing unrobust suggestions that ignore other possibilities and providing a more solid presentation of the results. Furthermore, several parts of the figures appear to be misread due to inadequate representation. We recommend providing appropriate evidence to improve the overall section.

Response: We thank the reviewer for this constructive assessment of Result and discussion Section. In the revised manuscript, we have therefore reduced redundancy and streamlined (especially Section 3.1) by removing repeated statements and consolidating overlapping sentences, while retaining the key results. Where evidence is indirect, we have rephrased statements to be appropriately qualitative and non-exclusive, and we now explicitly acknowledge plausible alternative mechanisms. We have rechecked the interpretation of all figures referenced in Section 3 and revised the text where the previous wording could be read as misinterpreting the plotted quantities or their temporal/regime correspondence. In addition, we improved figure readability/representation where needed (including the revision to Fig. 4b as a new Fig. 5) to minimize ambiguity.

Specific Comments

Fig. 1: Please include the place names and ocean areas described in section 2.1 on the map whenever possible. Also, please indicate what the contrast in the figure represents (probably sea ice).

Response: Complied with.

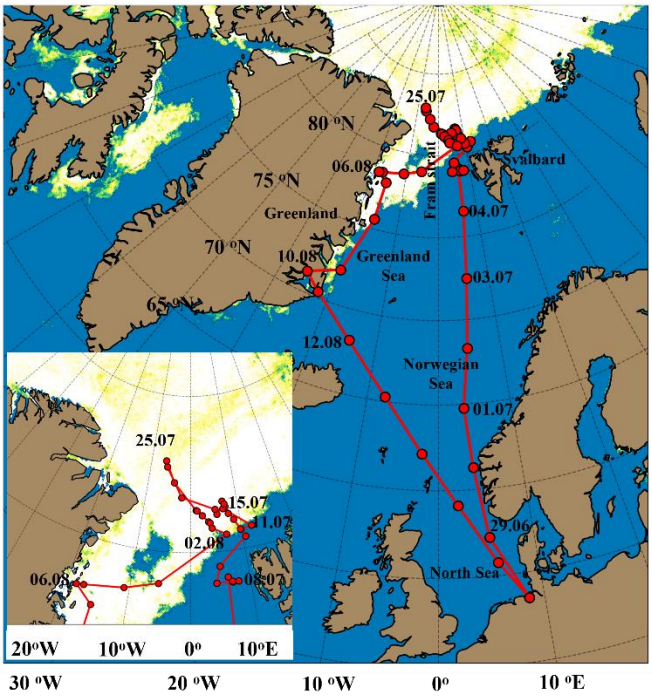

Figure 1: Ship track of RV Polarstern during the ATWAiCE cruise from 28 June to 17 August 2022. The red line indicates the cruise trajectory, with red circle symbols marking the ship's position at local noon each day. The inset shows a zoomed-in view of the northernmost cruise tracks. Background colour indicates Sea ice concentration (MODIS-AMSR2; Ludwig et al., 2020).

2.2: Variables should be in italics.

Response: Complied with.

L165 Volume equation: probably, 2CT or 2×CT, not 2xCT.

Response: Complied with.

The equation is corrected as:

The total volume of rBC containing particles at each grid point is estimated as (Yang et al. 2025),

$$Volume_{grid\ (i,j)} = \frac{\pi}{6} D_{p(i,j)}^{3} N_{i,j} = \frac{\pi}{6} (D_{c,i} + 2 \times CT_j)^3 N_{i,j}$$

3.1: σsca: Section 2 does not explain how this value was measured.

Response: Complied with. The following details are added to the revised manuscript in the section 2.2.

"The aerosol light scattering coefficient was measured using an integrating Nephelometer (Ecotech Aurora 4000). It measures the aerosol total scattering (σsca, between 10º and 170º) and back-scattering coefficients (between 90º and 170º) at three wavelengths (450, 525, and 635 nm). The nephelometer data was corrected following the methodology described by Müller et al. (2011). The detailed description of the main characteristics and the working principle of the integrating nephelometers can be found in Müller et al. (2011)."

Fig. 2: Faint and difficult to read, and the coloring of SE and NE is inconsistent.

Response: Complied with. The figure is corrected as follows;

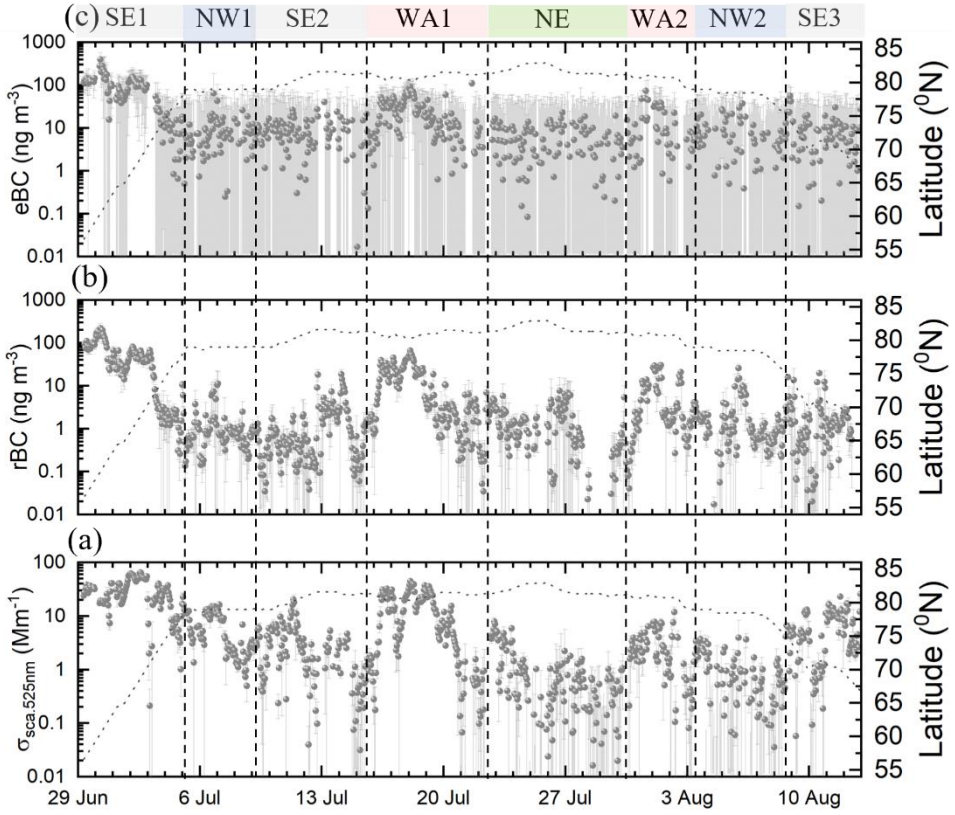

Figure 2: (a) Light scattering coefficient of aerosols measured at wavelength 525 nm using an integrating Nephelometer, (b) Refractory black carbon mass concentration measured using SP2, (c) Equivalent Black carbon mass concentration measured using MAAP. Each subplot is accompanied by a dotted line indicating the corresponding latitude (right y-axis). The vertical grey lines indicate the respective standard deviation for each parameter.

L264: If possible, please show the scattering plots between MrBC and eBC in a supplement, and clearly indicate the value below which eBC becomes unreliable.

Response: Complied with. The following figure is added to the Supplement.

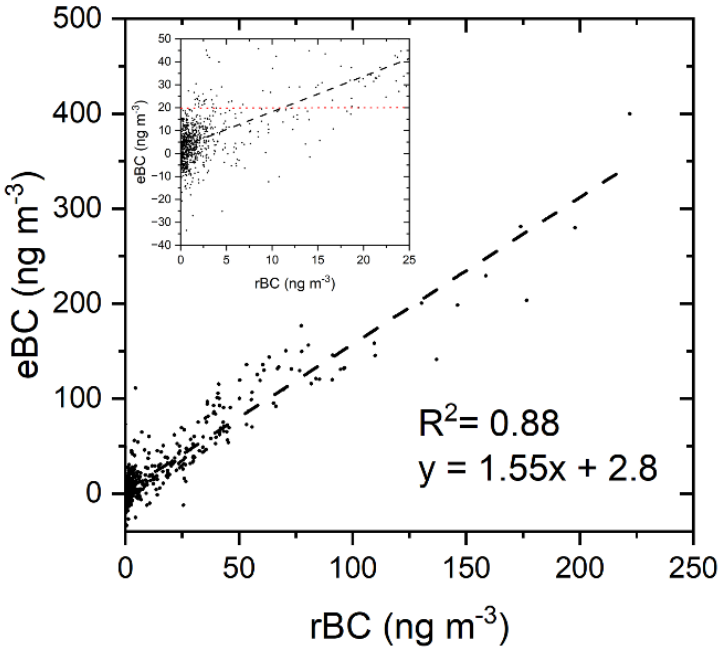

Figure S2: correlation between eBC measured by MAAP and rBC measured by SP2. Red dotted lines in the inset represents the value below which eBC becomes unreliable.

Fig. 3: The caption should also indicate that this is a 5-day trajectory.

Response: Complied with.

"Figure 3: 5-days backward airmass trajectories arriving at the ship position estimated using NOAA Hybrid Single-Particle Lagrangian Integrated Trajectory model (HYSPLIT) during the campaign segregated into different continuous airmass regimes (SE1- South easterly 1, NW1- North westerly 1, SE2- South easterly 2, WA1- Warm airmass intrusion 1, NE- North easterly, WA2- Warm airmass intrusion 2, NW2- North westerly 2, SE3- South easterly 3) during the study period."

Fig. 4b: It's difficult to read. Also, as I'll explain later, I recommend showing mass concentration rather than just mass fraction.

Response: Complied with. The Figure 4b is revised as a separate Figure 5 in the revised manuscript as shown here.

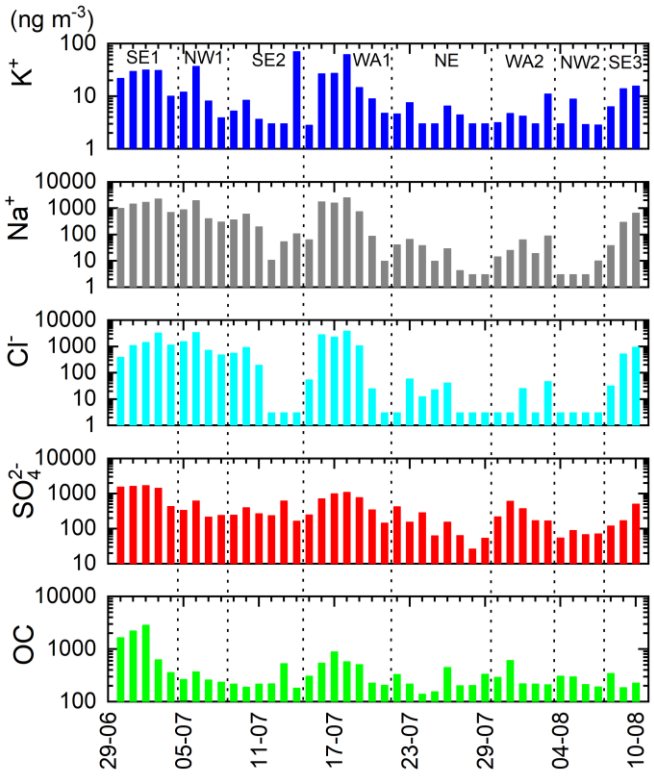

Figure 5: Mass concentration of major chemical species such as OC, SO_4^{2-}, Cl^-, Na^+ and K^+ measured during the study period.

Fig. 4c, d Polluted, Near-pristine, Pristine, Warm air mass: It would be better to explain these observation days in Sec. 2.1 or 3.1 to clarify the correspondence between these and Fig. 1.

Response: Complied with. The following details are added to the Section 3.1.

"The Polluted, Near-pristine, Pristine, Warm air mass classifications were made based on the aerosol loading and airmass histories during the campaign. The aerosol measurements 29 June to 05 of July close to the European continental regions is marked as 'polluted' whereas the observations during the NW1, NW2 and SE3 during 05-09 July, 03-12 August is marked as 'near pristine' and observations during 09-15 July and 22-30 July is marked as 'pristine'. The measurements during warm airmass intrusion period of 15-22 July and 30 July-03 August is marked as WA1 and WA2."

L310, L323, etc.: Regarding the comparison of σsca and Fig. 4b: The discussion of comparisons is often unconvincing because it fails to account for important aerosol factors, such as particle size, number, and concentration. For example, under conditions where BC from urban areas is high, it is assumed that secondary particles such as SO4 and OC will also be high. Generally, Na and Cl are generally coarse particles, while SO4 and OC are often fine particles. Fine particles, which are numerous and close to the wavelength of scattered light, scatter light efficiently, so they can contribute significantly to σsca even if they have a mass similar to that of coarse particles. Unfortunately, the particle composition was not classified by

particle size in this observation. However, I recommend at least discussing this as a concentration, not just as a mass fraction. It may also be effective to create a line graph by separating each component rather than stacking them. However, it would be easier to read if you just showed the results without making any unnecessary suggestions in the text.

Response: We thank the reviewer for this detailed and technically important comment. We agree that interpreting variations in the light scattering coefficient (σ_{sca}) using only bulk PM_{10} mass fractions can be unconvincing if particle size distribution, number, and mass concentration are not explicitly considered. As the reviewer notes, species typically associated with coarse mode (e.g., sea-salt-related Na and Cl) can contribute substantial mass but may be less efficient scatterers per unit mass at visible wavelengths than abundant fine-mode particles, whereas sulfate and organic aerosol are often enriched in the fine mode and can contribute significantly to σ_{sca}.

In the revised manuscript, we have therefore added an explicit limitation statement that our filter chemistry is PM_{10}, 24-h integrated, and not size-resolved; therefore, we cannot quantitatively apportion σ_{sca} by chemical component or size mode in this dataset. Following the reviewer suggestion, we show each major component as a separate time series (Figure 5) (rather than relying on a stacked representation), and we reduce speculative statements so the text primarily describes what is observed and what it is consistent with. In addition, we have reframed the σ_{sca} discussion with chemical composition such as sulfate/OC and sea-salt indicators are presented as contextual, explicitly noting that scattering depends strongly on particle size/number and not only on bulk mass fraction.

The following text is added to the revised manuscript.

"Interpretation of σ_{sca} variability based solely on PM_{10} bulk chemical composition is inherently qualitative because aerosol light scattering depends strongly on particle size distribution and number concentration, not only on mass fraction. In particular, coarse-mode constituents (e.g., Na^+ and Cl^-) may dominate mass during marine influence, whereas fine-mode sulfate and organic aerosol can contribute significantly to σ_{sca}. Since, our chemical composition of PM10 samples represents bulk, 24-h integrated composition across a broad size range, the discussion of it with respect to σ_{sca} is qualitative; scattering depends strongly on particle size distribution and number concentration, and we therefore do not attempt size or component resolved attribution with this."

L314 "SE3 trajectories, although marine-dominated, originated from the northern Atlantic sector, including the Barents and Norwegian Seas. ..." This is unsubstantiated. This result shows that SE2 and SE3 are clean, with no significant difference in MrBC, and that their trajectories are not significantly different.

Response:

We thank the reviewer for this important comment. We agree that our earlier text over-interpreted the origin and potential source influence of the SE3 regime. In

particular, the previous statement suggesting possible background European outflow or shipping influence was not sufficiently supported by the trajectory and composition data and has therefore been removed.

L390: The increase in K+ in Fig. 4b is unclear. I recommend including a time series graph in the supplement.

Response: Complied with. The mass concentration of K^+ is added to the revised Figure 5 along with other major species.

L438 "...This increase in MMD suggests a reduced influence from fossil fuel sources and a dominant role for biomass burning emissions in the central Arctic region via long-range atmospheric transport." This is unsubstantiated. As the author notes in the following paragraph, MMD in remote areas may change not only due to emission sources, but also due to changes during transport, such as removal and coagulation. Coagulation via clouds without precipitation may also effectively shift BC size significantly. I also think there are clear factors behind the small BC in SE1 and the large BC in WA1. However, for the rest cases, there is no support reason to suggest that the contribution of biomass burning is greater than that of transport processes.

Response: We thank the reviewer for pointing out this important point and agree that our original statement attributing the increase in MMD primarily to a "dominant role for biomass burning emissions" was not sufficiently supported by the evidence presented. We also agree that rBC core size in remote regions can evolve substantially during transport due to atmospheric processing, including preferential removal, cloud processing (with or without precipitation), and coagulation/aging-related shifts in the surviving rBC size distribution. Therefore, while the smaller MMD observed in SE1 is consistent with stronger fossil-fuel influence (as supported by the European outflow pathways and literature values), the progressive increase in MMD toward the central Arctic cannot be uniquely interpreted as a source-type transition without independent biomass-burning tracers or additional constraints.

In the revised manuscript, we have therefore removed the unsubstantiated claim that the observed MMD increase implies a dominant biomass-burning contribution in the central Arctic, reframed the latitudinal MMD increase as being consistent with a combination of changing source influence and transport/processing effects, explicitly acknowledging that these processes are not separable with the present dataset; and added an explicit sentence noting that cloud processing/coagulation and selective removal can shift MMD during long-range transport, potentially contributing to the observed pattern even under broadly similar source mixtures.

Accordingly, we have revised the MMD discussion as follows:

"Figure 7 shows the mass size distributions of rBC particles for the different airmass regimes during the cruise. The size distribution of rBC is relevant for

interpreting its atmospheric processing and radiative effects, as the light absorption properties of BC depend on core size, while the observed mass median diameter (MMD) can be influenced by source characteristics as well as by aging and removal during transport (Shiraiwa et al., 2007; McMeeking et al., 2010; Liu et al., 2014; Taylor et al., 2014; Kompalli et al., 2020, 2021; Yang et al., 2025).

The estimated MMD varied substantially across the different transport regimes. During SE1, the MMD was ~156 nm, i.e., the lowest among all regimes in this study. This value lies within the range commonly reported for polluted environments influenced by fossil fuel combustion, although such comparisons should be interpreted cautiously because the observed size distribution at the receptor site reflects not only source emissions but also atmospheric processing during transport (Laborde et al., 2013; Liu et al., 2019; Kompalli et al., 2020; Lim et al., 2023). As the ship moved away from the lower-latitudes towards the central Arctic, the MMD increased progressively; to ~ 190 nm during NW1, ~207 nm during SE2, and ~ 225 nm during NE. During NW2 and SE3, the MMD remained similarly larger, at ~217 nm and ~218 nm, respectively. These observations of MMD indicate a systematic increase in rBC core size from the lower-latitudes towards the central Arctic regimes. However, this gradient should not be interpreted as a unique fingerprint of changing emission sources. In remote regions, rBC size distributions can be modified during transport by size-dependent removal and atmospheric processing, including cloud processing and coagulation (Pan et al., 2026). Therefore, in the absence of independent source-specific tracers and high-resolution chemical composition information, the increase in MMD towards higher latitudes is interpreted here as reflecting the combined effects of distinct sources and atmospheric processing rather than as direct evidence of a transition to a specific source type.

A pronounced enhancement in MMD was observed during the warm airmass intrusion regime WA1, for which the estimated MMD was higher than 260 nm. This value is substantially larger than those observed during the background central Arctic regimes and coincided with enhanced rBC mass concentrations during the same period. As discussed in Section 3.2, WA1 was associated with transport from lower-latitude source regions along with the evidence for biomass burning influence. In contrast, during WA2, the MMD remained close to 220 nm, comparable to the values observed during the central Arctic background conditions. This difference between WA1 and WA2 further indicates that warm airmass intrusions into the central Arctic do not exert a uniform influence on the microphysical characteristics of rBC; rather, their effect on rBC size distribution depends on the transport pathways and the atmospheric processing within the advected airmass.

Changes in MMD during long-range atmospheric transport can arise from multiple competing processes. Size dependent wet removal may preferentially remove larger BC containing particles under some conditions and thereby shift the distribution towards smaller diameters (Moteki et al., 2012; Schulz et al., 2019). Conversely, coagulation and condensational aging may increase the

apparent characteristic size of BC containing particles or preferentially preserve larger cores under specific transport conditions (Tunved et al., 2013; Schulz et al., 2019). The observed MMD thus reflects the combined influence of source emissions, removal, and atmospheric processing. This is particularly relevant in the Arctic, where transport pathways, cloud interactions, and scavenging processes jointly control the abundance and properties of BC reaching the central Arctic atmosphere (Liu et al., 2011; Schulz et al., 2019).”

Sec. 3.4 Fig. 7 and paragraphs 1, 2, and 3: The color bars are shown as a % of max., so the contrast varies depending on the maximum values. This can lead to many misinterpretations. For example, L483 "It is interesting to note a higher volume of rBC with core sizes >150 nm, except for SE2 and SE3." The overall low contrast in the SE2 and SE3 figures is likely because the used max. values were high. Probably, SE2 and SE3, like other air masses, also have a relatively higher volume of rBC with core sizes >150 nm. This figure makes it unclear what is being compared (are large cores being compared to small cores, or absolute values for each air mass?). If discussing absolute values (particle volume concentration), we recommend using a color bar with units of nm3/m3 for each figure. If discussing relative distributions, we recommend redrawing the distribution normalized by the integrated volume (not maximum). I would like you to check your interpretation of section 3.4 as a whole to ensure there are no errors.

Response: We thank the reviewer for this important and constructive comment. Following the reviewer’s suggestion, we have revised Fig. 7 by normalizing the distributions to the integrated rBC volume rather than to the maximum value. This revised representation more clearly highlights the relative contribution of different rBC core-size ranges within each air mass and avoids potentially misleading contrasts arising from differences in peak magnitudes. We agree that this approach is more appropriate for Sect. 3.4, where the aim is to compare the relative characteristics of the size distributions in each airmass regimes rather than absolute volume concentrations.

In addition, we have carefully re-evaluated the interpretation presented throughout Sect. 3.4, including the discussion associated with Fig. 7 and to ensure that the conclusions are fully consistent with the revised figure. The corresponding text has been updated accordingly to improve clarity and avoid possible misinterpretation.

The Figure and the text are revised as follows;

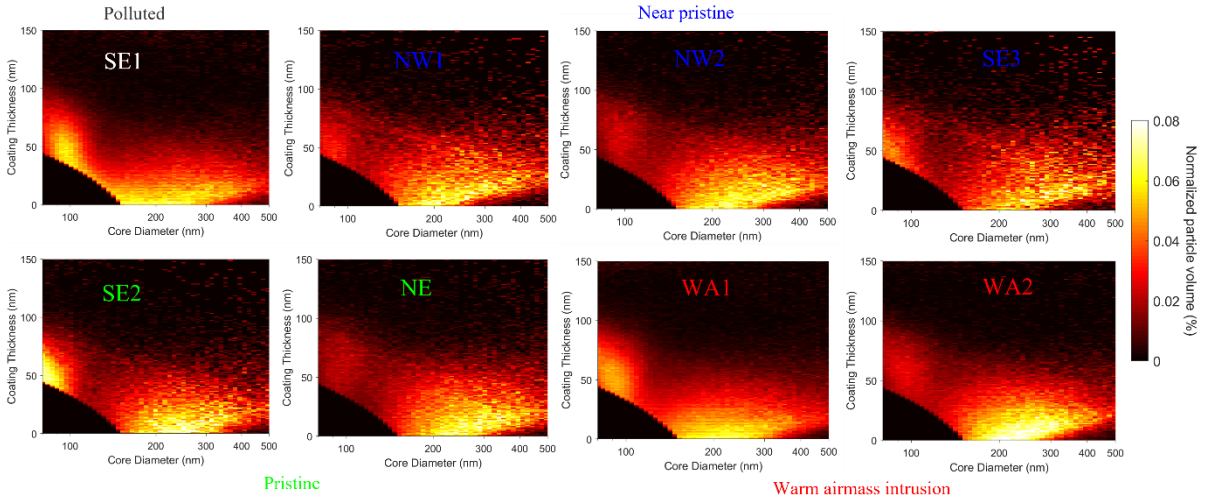

Figure 8: Size segregated coating thickness of rBC particles during the campaign. The colour bar indicates the particle volume normalized with the integrated total volume (in %) in each size bin.

Figure 8 shows the size resolved coating thickness of rBC particles estimated during the study period, along with the normalized rBC particle volume. The size resolved coating thickness (CT) of rBC particles, along with the number concentration of particles is given in the supplementary Figure S5. This size-resolved CT classification provided a more direct insight into the mixing state of rBC particles in this study. It is evident that, throughout the study period, two distinct regions (below Dc~150 nm and above Dc~150 nm) consistently exhibited relatively higher volume of coated rBC. This suggests that the rBC population during the campaign was characterized by pronounced mixing-state heterogeneity. The repeated occurrence of two enhanced-volume domains, one associated with smaller cores and another with larger cores, indicates that non-BC material was distributed unevenly across the rBC population, with some particles remaining weakly processed while others acquired substantial coatings. This particle-to-particle variability is important because the radiative effects of rBC depends not only on the mean coating thickness, but also on how the coating is distributed among particles of different core sizes, as emphasized in recent studies (Fierce et al., 2016, 2020; Zeng et al., 2024; Zhai et al., 2022).

The higher contribution from coated larger rBC cores under the northerly and near-pristine regimes likely reflects aged, internally mixed particles that underwent substantial atmospheric processing during long-range transport to the central Arctic. In remote marine environments previous studies reported larger rBC cores with thick coating (Pan et al., 2026). In this study, we found the relatively higher coated volume observed at both smaller and larger cores during SE2 and WA1 points to a broader spread of core-shell combinations, implying a more diverse and complex mixing state under those regimes in the Arctic. Such a pattern suggests that, in addition to aged large-core particles, a greater fraction of smaller rBC cores had also acquired sufficient condensed material to become internally mixed. Condensational aging generally enhances coating accumulation more efficiently on smaller BC cores than on larger ones

(Seinfeld and Pandis, 2006). The bottom-left region with null values corresponds to smaller rBC particles that show neither positive nor negative coating thickness (CT), due to the detection limitations of the SP2, as reported in several studies (Ko et al., 2020; Yang et al., 2025). This detection limitation restricts the retrieval of coating information from scattered light for smaller rBC particles. As a result, the mixing state information of a substantial portion of these smaller rBC particles remains unresolved. This missing fraction of CT results in overestimation of CT when estimating the absolute coating thickness across the entire size range.

Sec. 3.4 Fig. 8 and paragraphs 4, 5, 6, and 7: I found the discussion of the relationship between air masses and CT interesting. While I don't strongly recommend it, have you considered the relationship between particle number concentration (e.g., scattering particles measured by a SP2) and CT as a factor determining CT? For example, in cases like WA1, where particle number concentration is high, even if precursor gas is present, secondary products may be distributed among many particles, preventing a thick CT.

Response:

We thank the reviewer for this thoughtful suggestion. We agree that particle number concentration can, in principle, influence the evolution of coating thickness (CT) by regulating how available condensable material is partitioned across the particle population. Under high number concentration conditions, condensable products may be distributed among more particles, which can limit coating thickness per particle even when precursor gases are present, an effect that could be relevant for regimes such as WA1.

In the present study, however, our dataset does not provide a sufficiently constrained measure of the total population of potential "condensation sinks" across the full aerosol size distribution, nor a direct way to quantify precursor availability and its allocation among particles. The SP2-derived number concentrations represent BC-containing particles within the SP2 detection range and do not capture the full abundance of scattering/non-BC particles that also compete for condensable vapours. Therefore, while the proposed mechanism is physically plausible, we cannot robustly test or quantify it with the current observations.

To incorporate the reviewer's point without overreaching, we have added a brief, explicitly qualified statement in Section 3.4 noting that (in addition to transport history and source-related factors) variations in particle number/condensation sink may modulate CT, particularly during high-loading regimes, but that a quantitative assessment would require size-resolved number distributions and/or gas-phase precursor measurements.

Text added to the revised manuscript:

"Coating thickness may also be modulated by the available condensation sink. Under high particle number conditions, condensable material can be distributed across a larger population, potentially limiting per-particle coating growth even

when precursors are present. Although we cannot quantify this effect here because SP2 number concentrations represent only BC-containing particles within the instrument's detection range (and not the full aerosol population), this mechanism could also contribute to the relatively low CT observed during high loading regimes such as WA1."

3.5: As mentioned in the major comment, there are many previous studies on Eabs, including observational results and model calculations, and it is best to consider that values calculated using the core-shell assumption have limited utility. I recommend confirming the Eabs values observed in previous studies relative to the overlying pressure and discussing the range of values that can be used to interpret this study.

Response: We thank the reviewer for this important suggestion. In the revised manuscript, we have expanded the discussion of the estimated absorption enhancement factor (E_{abs}) and placed our results in the context of previous observational and modeling studies. We now explicitly acknowledge that the core-shell Mie method provides an upper-bound estimate of absorption enhancement because it assumes a fully encapsulated spherical BC core, whereas ambient rBC particles often exhibit irregular morphology, partial coating, and substantial particle-to-particle heterogeneity in mixing state. To address the reviewer's concern, we have compared our estimated E_{abs} values with those reported in previous field and laboratory studies. In addition, we have incorporated the E_{abs} and MAC values from previous studies in Figure 10. In addition, tables showing the comparisons with other field studies and methodologies used are provided in supplementary details.

We have added the following discussion in the revised manuscript.

"It is worth noting that the estimated E_{abs} values in this study are comparable with earlier field observations, including ~1.06 in California (Cappa et al., 2012), ~1.06 at an east Asian outflow site Noto Peninsula (Ueda et al., 2016), ~1.38 during biomass burning events in Boulder (Lack et al., 2012), 1.50 ± 0.48 in the Pearl River Delta (Wu et al., 2018), ~1.36 for marine airmass periods to ~1.58 for the continental airmass periods over a tropical coastal site (Nithin et al., 2026), ~ 1.15 in Beijing (Liu et al., 2020), and ~1.69 in Shanghai (Zhai et al., 2022), ~1.42 Nanjing in China (Ma et al., 2020), 1.1-1.3 in a background site in the Qinghai-Tibet Plateau (Zeng et al. 2024). Larger values approaching or exceeding 2 have been observed in strongly aged or biomass-burning-influenced aerosol, such as pyrocumulonimbus plumes and remote high-altitude environments (Beeler et al., 2024; Tinorua et al., 2024). Zhang et al. (2023) also reported E_{abs} in the range of ~1.2-2.0 with higher E_{abs} for fully coated BC in North China Plain. Utilizing the global measurements, Asmi et al., (2025; and references therein) reported average E_{abs} for the urban and remote environments as 1.38 and 1.59 respectively as well as Eabs ~1.8-3.0 for the biomass burning smoke. Laboratory evidence also indicates that coatings can substantially enhance BC absorption. Shiraiwa et al. (2010) found an approximately 2-fold increase in absorption for BC coated with oleic acid and glycerol, while Khalizov et al. (2009) reported an

Eabs of around 1.4 after sulfuric acid condensation on black carbon. These previous studies collectively indicate that most atmospheric E_{abs} values fall in the range of about 1.0-2.0 under typical ambient conditions, while higher values are generally associated with extensive aging, thicker coatings, or biomass-burning influence. It is important to note, however, that E_{abs} values reported in the literature are derived using different methodological approaches, including core-shell Mie theory, thermodenuder coupled with photoacoustic absorption measurements, filter-based methods, and optical approaches combining cavity ring-down spectroscopy and nephelometry. Similarly, MAC values have been derived using different combinations of absorption measurements and BC mass quantification, such as PSAP or photoacoustic absorption together with EC, SP2, SP-AMS, or COSMOS measurements. These methodological differences can contribute to inter-study variability and should be considered when comparing absolute values across regions and source regimes. Table S1 and Table S2 providing an overview of the E_{abs} and MAC values and methods used in previous studies. It is important to note that the E_{abs} values reported here are based on a core-shell Mie theory that assumes a spherical BC core fully encapsulated by non-absorbing coating material. Ambient rBC particles, however, often exhibit fractal/irregular morphologies, partial coating, and mixing state heterogeneity. As a result, core-shell-based E_{abs} may represent an upper-bound or idealized estimate of absorption enhancement relative to more realistic particle representations (e.g., Adachi et al., 2010; Ueda et al., 2016; Fierce et al., 2020; Liu et al., 2020; Zhai et al., 2022; Romshoo et al., 2025). Overall, the present results indicate that most E_{abs} values in the central Arctic fall within the lower to moderate range reported for ambient atmospheric conditions, and that the variability between regimes is primarily controlled by the combined influence of source characteristics, atmospheric aging, and mixing state.

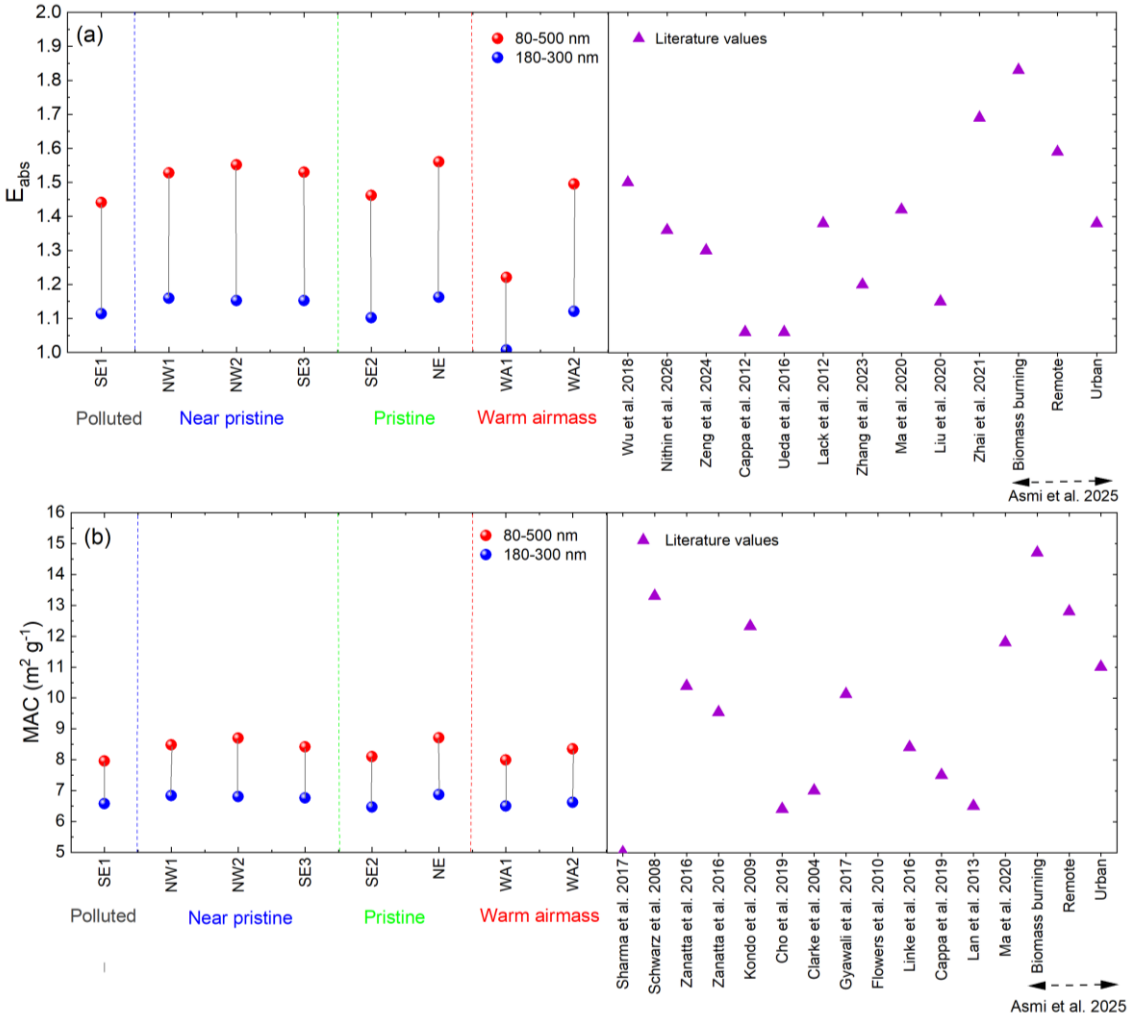

Figure 10: (a) Estimated absorption enhancement (E_{abs}) of refractory black carbon particles for each regime for the rBC core size ranges,80-500 nm and180-300 nm. (b) Estimated mass absorption cross section of refractory black carbon particles for each regime for the rBC core size ranges,80-500 nm and 180-300 nm.

Table S1: Summary of previously reported light absorption enhancement values (E_{abs}) for black carbon from different environments.

E_{abs}	Wavelength (nm)	Location	Method	Reference
1.0-1.6	550	Arctic	Core-shell Mie theory	Present study
1.5	550	Pearl River Delta, China	Filter based with minimum R-squared method	Wu et al. (2018)
1.36	550	Thumba	Core-shell Mie theory	Nithin et al. (2026)
1.3	550	Qinghai-Tibet Plateau	Core-shell Mie theory	Zeng et al. (2024)
1.06	532	California, USA	Thermodenuder + photoacoustic absorption method	Cappa et al. (2012)

1.06	532	Noto Peninsula, Japan	Thermodenuder + photoacoustic absorption method	Ueda et al. (2016)
1.38	532	Boulder, Colorado, USA	Thermodenuder + photoacoustic absorption method	Lack et al. (2012)
1.2	550	Xianghe, North China Plain, China	Core-shell Mie theory	Zhang et al. (2023)
1.42	532	Nanjing, China	Thermodenuder + photoacoustic absorption method	Ma et al. (2020)
1.15	550	Beijing, China	Core-shell Mie theory	Liu et al. (2020)
1.69	532	Shanghai, China	TD-CRDS/nephelometer	Zhai et al. (2021)
1.83	550	Biomass burning, multiple sites/global synthesis	Filter-photometer-based compilation	Asmi et al. (2025)
1.59	550	Remote, multiple sites/global synthesis	Filter-photometer-based compilation	Asmi et al. (2025)
1.38	550	Urban, multiple sites/global synthesis	Filter-photometer-based compilation	Asmi et al. (2025)

Table S2: Summary of previously reported mass absorption cross-section values of black carbon from different environments.

MAC	Wavelength (nm)	Location	Method	Reference
6.5-8.7	550	Arctic	Core-shell Mie theory	Present study
5	550	Alert, Canada	Particle soot absorption photometer with EC and SP2	Sharma et al. (2017)
13.3	530	Texas, USA	Particle soot absorption photometer with SP2	Schwarz et al. (2008)
10.38	522	Aspvreten, Sweden	Particle soot absorption photometer with EC	Zanatta et al. (2016)
9.54	525	Birkenes, Norway	Particle soot absorption photometer EC	Zanatta et al. (2016)
12.32	565	Jeju Island, Korea	Particle soot absorption photometer with EC	Kondo et al. (2009)
6.4	565	Gosan Climate Observatory	COSMOS with EC	Cho et al. (2019)
7	565	ACE-Asia, C-130 flights below 2km	Particle soot absorption photometer with EC	Clarke et al. (2004)

10.12	532	Cool, USA	Photoacoustic spectrometer with SP2	Gyawali et al. (2017)
3.1	532	Jeju Island, Korea	Photoacoustic spectrometer with EC	Flowers et al. (2010)
8.4	532	Karlsruhe, Germany	photoacoustic absorption + SP2	Linke et al. (2016)
7.5	532	California, USA	Photoacoustic absorption + SP2 rBC mass	Cappa et al. (2019)
6.5	532	South China	Photoacoustic absorption + SP2 rBC mass	Lan et al. (2013)
11.8	532	Nanjing, China	Photoacoustic soot spectrometer + SP-AMS	Ma et al. (2020)
14.7	550	Biomass burning, multiple sites/global synthesis	Filter-photometer-based compilation	Asmi et al. (2025)
12.8	550	Remote, multiple sites/global synthesis	Filter-photometer-based compilation	Asmi et al. (2025)
11	550	Urban, multiple sites/global synthesis	Filter-photometer-based compilation	Asmi et al. (2025)

Conclusion: I recommend reorganizing the section based on the above corrections.

Response: The conclusion section is revised as follows.

To investigate the microphysical properties and mixing state of atmospheric refractory black carbon (rBC) particles in the central Arctic marine boundary layer, measurements were conducted on board RV *Polarstern* during the ATWAICE campaign in summer 2022. This study provides new insights into the spatial and temporal variability of rBC properties including its abundance, size distribution, mixing state, and radiative properties during the summer melt season. Our results reveal that airmass transport pathways and atmospheric processing strongly influence rBC abundance, its size distribution, and mixing state in the summertime central Arctic marine boundary layer. rBC mass concentrations, size distributions, and coating thickness varied substantially across the different transport regimes considered in this study. The lowest rBC mass concentrations were observed under pristine and near-pristine conditions, typically on the order of ~0.4- 0.6 ng m^{-3}. In contrast warm airmass intrusions into the central Arctic were associated with clear enhancements in rBC, with maximum concentrations reaching ~74 ng m^{-3} during WA1. These results demonstrate that episodic transport from lower latitudes can strongly perturb the otherwise low-aerosol summertime Arctic background. Further, the higher rBC during WA1 is found to associated with significant influences from the biomass burning sources during the warm airmass intrusion.

The mass median diameter (MMD) of rBC varied substantially across the different transport regimes with a clear latitudinal shift in the mass median diameter (MMD) of rBC from the lower latitude near coastal marine environments (~156 nm) to the high latitudes of the central Arctic (~220 nm). The particularly high MMD observed during WA1 (>260 nm) indicates that warm-air intrusions can substantially modify the microphysical properties of rBC in the central Arctic. The observed variability in MMD is interpreted as reflecting the combined effects of source influence, airmass transport pathways, and atmospheric processing during long-range transport, rather than a unique signature of emission source alone. The mixing state of rBC showed similarly strong regime dependence. The size-resolved mixing state revealed pronounced heterogeneity, with non-BC material distributed unevenly across rBC particles of different core sizes. Airmasses with higher continental influence generally exhibited enhanced rBC concentrations and distinct coating characteristics relative to the clean marine and sea-ice influenced regimes. At the same time, the observed coating thickness were often lower than that might be expected for aged particles transported over long distances.

The size-resolved analysis of light absorption properties based on the core-shell Mie theory further showed substantial variability in both the absorption enhancement (E_{abs}) and the mass absorption cross-section (MAC). The size-resolved E_{abs} values ranged from approximately 1.0 - 1.6 across all airmass regimes. The pristine and near-pristine regimes exhibited comparatively high E_{abs} and MAC values, consistent with more internally mixed and atmospherically processed particles. In contrast, WA1 showed comparatively low E_{abs} (generally <1.1) despite enhanced rBC concentrations, indicating that the particles transported during this event were not necessarily highly coated. By comparison, WA2 exhibited higher E_{abs} than WA1, with weaker evidence of direct combustion influence. This contrast indicates that the radiative properties of rBC in the Arctic are governed not only by source region but also by airmass transport pathways, as passage over marine or relatively cleaner environments may promote prolonged aging and a greater influence of secondarily processed aerosol on the mixing state of rBC.

Our results highlight the strong spatial and temporal variability of rBC microphysical and optical properties in the summer Arctic marine boundary layer. The results emphasize that fixed or generalized MAC or E_{abs} are unlikely to adequately represent Arctic conditions. Instead, regime-specific and size-resolved representations that account for mixing state and atmospheric aging conditions are needed to improve model descriptions of BC radiative effects in the Arctic. Given the high climatic sensitivity of the Arctic to light absorbing aerosols perturbations, improved characterization of rBC abundance, size and mixing state heterogeneity is essential for reducing uncertainties in estimates of aerosol radiative forcing and Arctic climate projections.

References:

Adachi, K., Chung, S. H., and Buseck, P. R.: Shapes of soot aerosol particles and implications for their effects on climate, Journal of Geophysical Research Atmospheres, 115, https://doi.org/10.1029/2009JD012868, 2010.

Beeler, P., Kumar, J., Schwarz, J. P., Adachi, K., Fierce, L., Perring, A. E., Katich, J. M., and Chakrabarty, R. K.: Light absorption enhancement of black carbon in a pyrocumulonimbus cloud, Nature Communications, 15, https://doi.org/10.1038/s41467-024-50070-0, 2024.

Cappa, C. D., Onasch, T. B., Massoli, P., Worsnop, D. R., Bates, T. S., Cross, E. S., Davidovits, P., Hakala, J., Hayden, K. L., Jobson, B. T., Kolesar, K. R., Lack, D. A., Lerner, B. M., Li, S. M., Mellon, D., Nuaaman, I., Olfert, J. S., Petäjä, T., Quinn, P. K., Song, C., Subramanian, R., Williams, E. J., and Zaveri, R. A.: Radiative absorption enhancements due to the mixing state of atmospheric black carbon, Science (1979)., 337, 1078–1081, https://doi.org/10.1126/science.1223447, 2012.

Cappa, C. D., Zhang, X., Russell, L. M.,Collier, S., Lee, A. K. Y., Chen, C.-L., etal. (2019). Light absorption by ambientblack and brown carbon and itsdependence on black carbon coatingstate for two California, USA, cities inwinter and summer. Journal ofGeophysical Research: Atmospheres,124, 1550–1577. https://doi.org/10.1029/2018JD029501.

Cho, C., Kim, S. W., Lee, M., Lim, S., Fang, W., Gustafsson, Ö., Andersson, A., Park, R. J., and Sheridan, P. J.: Observation-based estimates of the mass absorption cross-section of black and brown carbon and their contribution to aerosol light absorption in East Asia, Atmos. Environ., 212, 65–74, https://doi.org/10.1016/j.atmosenv.2019.05.024, 2019.

Clarke, A. D., Shinozuka, Y., Kapustin, V. N., Howell, S., Huebert, B., Doherty, S., Anderson, T., Covert, D., Anderson, J., Hua, X., Moore, K. G., McNaughton, C., Carmichael, G., and Weber, R.: Size distributions and mixtures of dust and black carbon aerosol in Asian outflow: Physiochemistry and optical properties, Journal of Geophysical Research D: Atmospheres, 109, https://doi.org/10.1029/2003JD004378, 2004.

Flowers, B. A., Dubey, M. K., Mazzoleni, C., Stone, E. A., Schauer, J. J., Kim, S. W., and Yoon, S. C.: Optical-chemical-microphysical relationships and closure studies for mixed carbonaceous aerosols observed at Jeju Island; 3-laser photoacoustic spectrometer, particle sizing, and filter analysis, Atmos. Chem. Phys., 10, 10387–10398, https://doi.org/10.5194/acp-10-10387-2010, 2010.

Fossum, K. N., Ovadnevaite, J., Liu, D., Flynn, M., O'Dowd, C., and Ceburnis, D.: Background levels of black carbon over remote marine locations, Atmos. Res., 271, https://doi.org/10.1016/j.atmosres.2022.106119, 2022.

Gyawali, M., Arnott, W. P., Zaveri, R. A., Song, C., Flowers, B., Dubey, M. K., Setyan, A., Zhang, Q., China, S., Mazzoleni, C., Gorkowski, K., Subramanian, R., and Moosmüller, H.: Evolution of multispectral aerosol absorption properties in a biogenically-influenced urban environment during the CARES campaign, Atmosphere (Basel)., 8, https://doi.org/10.3390/atmos8110217, 2017.

Khalizov, A. F., Xue, H., Wang, L., Zheng, J., and Zhang, R.: Enhanced light absorption and scattering by carbon soot aerosol internally mixed with sulfuric acid, Journal of Physical Chemistry A, 113, 1066–1074, https://doi.org/10.1021/jp807531n, 2009.

Kondo, Y., Sahu, L., Kuwata, M., Miyazaki, Y., Takegawa, N., Moteki, N., Imaru, J., Han, S., Nakayama, T., Oanh, N. T. K., Hu, M., Kim, Y. J., and Kita, K.: Stabilization of the mass absorption cross section of black carbon for filter-based absorption photometry by the use of a heated inlet, Aerosol Science and Technology, 43, 741–756, https://doi.org/10.1080/02786820902889879, 2009.

Lack, D. A., Langridge, J. M., Bahreini, R., Cappa, C. D., Middlebrook, A. M., and Schwarz, J. P.: Brown carbon and internal mixing in biomass burning particles, 109, 14802–14807, https://doi.org/10.1073/pnas.1206575109/-/DCSupplemental, 2012.

Lan, Z. J., Huang, X. F., Yu, K. Y., Sun, T. Le, Zeng, L. W., and Hu, M.: Light absorption of black carbon aerosol and its enhancement by mixing state in an urban atmosphere in South China, Atmos. Environ., 69, 118–123, https://doi.org/10.1016/j.atmosenv.2012.12.009, 2013.

Linke, C., Ibrahim, I., Schleicher, N., Hitzenberger, R., Andreae, M. O., Leisner, T., and Schnaiter, M.: A novel single-cavity three-wavelength photoacoustic spectrometer for atmospheric aerosol research, Atmos. Meas. Tech., 9, 5331–5346, https://doi.org/10.5194/amt-9-5331-2016, 2016.

Liu, D., Flynn, M., Gysel, M., Targino, A., Crawford, I., Bower, K., Choularton, T., Juňnyi, Z., Steinbacher, M., Ḧglin, C., Curtius, J., Kampus, M., Petzold, A., Weingartner, E., Baltensperger, U., and Coe, H.: Single particle characterization of black carbon aerosols at a tropospheric alpine site in Switzerland, Atmos. Chem. Phys., 10, 7389–7407, https://doi.org/10.5194/acp-10-7389-2010, 2010.

Liu, H., Pan, X., Liu, D., Liu, X., Chen, X., Tian, Y., Sun, Y., Fu, P., and Wang, Z.: Mixing characteristics of refractory black carbon aerosols at an urban site in Beijing, Atmos. Chem. Phys., 20, 5771–5785, https://doi.org/10.5194/acp-20-5771-2020, 2020.

Liu, S., Aiken, A. C., Gorkowski, K., Dubey, M. K., Cappa, C. D., Williams, L. R., Herndon, S. C., Massoli, P., Fortner, E. C., Chhabra, P. S., Brooks, W. A., Onasch, T. B., Jayne, J. T., Worsnop, D. R., China, S., Sharma, N., Mazzoleni, C., Xu, L., Ng, N. L., Liu, D., Allan, J. D., Lee, J. D., Fleming, Z. L., Mohr, C., Zotter, P., Szidat, S., and Prévôt, A. S. H.: Enhanced light absorption by mixed source black and brown carbon particles in UK winter, Nat. Commun., 6, https://doi.org/10.1038/ncomms9435, 2015.

Ma, Y., Huang, C., Jabbour, H., Zheng, Z., Wang, Y., Jiang, Y., Zhu, W., Ge, X., Collier, S., and Zheng, J.: Mixing state and light absorption enhancement of black carbon aerosols in summertime Nanjing, China, Atmos. Environ., 222, https://doi.org/10.1016/j.atmosenv.2019.117141, 2020.

Nithin, B., Kompalli, S. K., and Babu, S. S.: Black carbon mixing state and light-absorption enhancement under different air mass regimes over a tropical coastal site, Atmos. Res., 331, https://doi.org/10.1016/j.atmosres.2025.108641, 2026.

Pan, X., Zhang, Y., Xue, C., Kuhn, U., Hrabe de Angelis, I., Pöhlker, C., Ditas, J., Heins, L., Aardema, H. M., Slagter, H. A., Calleja, M. Ll., Dragoneas, A., Walter, D., Nillius, B., Wang, Q., Ma, N., Su, H., Pöschl, U., Haug, G. H., Schiebel, R., and Cheng, Y.: Black Carbon in the Marine Atmosphere: Concentration and Mixing State From Coastal to Remote Atlantic Regions, Journal of Geophysical Research: Atmospheres, 131, https://doi.org/10.1029/2025JD045346, 2026.

Raatikainen, T., Brus, D., Hooda, R. K., Hyvarinen, A. P., Asmi, E., Sharma, V. P., Arola, A., and Lihavainen, H.: Size-selected black carbon mass distributions and mixing state in polluted and clean environments of northern India, Atmos. Chem. Phys., 17, 371–383, https://doi.org/10.5194/acp-17-371-2017, 2017.

Romshoo, B., Patil, J., Michels, T., Müller, T., Kloft, M., and Pöhlker, M.: Improving the predictions of black carbon (BC) optical properties at various aging stages using a machine-learning-based approach, Atmos. Chem. Phys., 24, 8821–8846, https://doi.org/10.5194/acp-24-8821-2024, 2024.

Seinfeld, J. H., & Pandis, S. N, Atmospheric chemistry and physics: From air pollution to climate change. John Wiley & Sons, Inc., 2006.

Sharma, S., Richard Leaitch, W., Huang, L., Veber, D., Kolonjari, F., Zhang, W., Hanna, S. J., Bertram, A. K., and Ogren, J. A.: An evaluation of three methods for measuring black carbon in Alert, Canada, Atmos. Chem. Phys., 17, 15225–15243, https://doi.org/10.5194/acp-17-15225-2017, 2017.

Shiraiwa, M., Kondo, Y., Moteki, N., Takegawa, N., Sahu, L. K., Takami, A., Hatakeyama, S., Yonemura, S., and Blake, D. R.: Radiative impact of mixing state of black carbon aerosol in Asian outflow, Journal of Geophysical Research Atmospheres, 113, https://doi.org/10.1029/2008JD010546, 2008.

Shiraiwa, M., Kondo, Y., Iwamoto, T., and Kita, K.: Amplification of light absorption of black carbon by organic coating, Aerosol Science and Technology, 44, 46–54, https://doi.org/10.1080/02786820903357686, 2010.

Tinorua, S., Denjean, C., Nabat, P., Bourrianne, T., Pont, V., Gheusi, F., and Leclerc, E.: Higher absorption enhancement of black carbon in summer shown by 2-year measurements at the high-altitude mountain site of Pic du Midi Observatory in the French Pyrenees, Atmos. Chem. Phys., 24, 1801–1824, https://doi.org/10.5194/acp-24-1801-2024, 2024.

Ueda, S., Nakayama, T., Taketani, F., Adachi, K., Matsuki, A., Iwamoto, Y., Sadanaga, Y., and Matsumi, Y.: Light absorption and morphological properties of soot-containing aerosols observed at an East Asian outflow site, Noto Peninsula, Japan, Atmos. Chem. Phys., 16, 2525–2541, https://doi.org/10.5194/acp-16-2525-2016, 2016.

Wang, Q., Cao, J., Han, Y., Tian, J., Zhu, C., Zhang, Y., Zhang, N., Shen, Z., Ni, H., Zhao, S., and Wu, J.: Sources and physicochemical characteristics of black carbon aerosol from the southeastern Tibetan Plateau: Internal mixing enhances light absorption, Atmos. Chem. Phys., 18, 4639–4656, https://doi.org/10.5194/acp-18-4639-2018, 2018.

Wang, Q. Y., Huang, R. J., Cao, J. J., Tie, X. X., Ni, H. Y., Zhou, Y. Q., Han, Y. M., Hu, T. F., Zhu, C. S., Feng, T., Li, N., and Li, J. D.: Black carbon aerosol in winter northeastern Qinghai-Tibetan Plateau, China: The source, mixing state and optical property, Atmos. Chem. Phys., 15, 13059–13069, https://doi.org/10.5194/acp-15-13059-2015, 2015.

Wang, Y., Li, W., Huang, J., Liu, L., Pang, Y., He, C., Liu, F., Liu, D., Bi, L., Zhang, X., and Shi, Z.: Nonlinear Enhancement of Radiative Absorption by Black Carbon in Response to Particle Mixing Structure, Geophys. Res. Lett., 48, https://doi.org/10.1029/2021GL096437, 2021.

Wu, C., Wu, D., and Zhen Yu, J.: Quantifying black carbon light absorption enhancement with a novel statistical approach, Atmos. Chem. Phys., 18, 289–309, https://doi.org/10.5194/acp-18-289-2018, 2018.

Wu, Y., Cheng, T., Liu, D., Allan, J. D., Zheng, L., and Chen, H.: Light Absorption Enhancement of Black Carbon Aerosol Constrained by Particle Morphology, Environ. Sci. Technol., 52, 6912–6919, https://doi.org/10.1021/acs.est.8b00636, 2018.

Zanatta, M., Gysel, M., Bukowiecki, N., Müller, T., Weingartner, E., Areskoug, H., Fiebig, M., Yttri, K. E., Mihalopoulos, N., Kouvarakis, G., Beddows, D., Harrison, R. M., Cavalli, F., Putaud, J. P., Spindler, G., Wiedensohler, A., Alastuey, A., Pandolfi, M., Sellegri, K., Swietlicki, E., Jaffrezo, J. L., Baltensperger, U., and Laj, P.: A European aerosol phenomenology-5: Climatology of black carbon optical properties at 9 regional background sites across Europe, Atmos. Environ., 145, 346–364, https://doi.org/10.1016/j.atmosenv.2016.09.035, 2016.

Zhang, Y., Su, H., Kecorius, S., Ma, N., Wang, Z., Sun, Y., Zhang, Q., Pöschl, U., Wiedensohler, A., Andreae, M. O., and Cheng, Y.: Extremely low-volatility organic coating leads to underestimation of black carbon climate impact, One Earth, 6, 158–166, https://doi.org/10.1016/j.oneear.2023.01.009, 2023.

Zhang, Z., Wang, J., Riemer, N., Liu, C., Wang, J., Jin, Y., Tian, Z., Chen, G., Wang, B., Huang, X., Ding, A., and Wang, S.: Inversion Approach for Inferring Mixing State and Improving Optical Estimation of Coated Black Carbon Using Bulk-Volume Variables and Number-Size Distributions, Environ. Sci. Technol., 60, 3998–4007, https://doi.org/10.1021/acs.est.5c10094, 2026.